Vortex sensing analysis of radially and pseudo-radially polarized beams

Jeffrey A. Davis
Don M. Cottrell
Brandon C. Schoonover
Johnathan B. Cushing
Jorge Albero
Ignacio Moreno

Vortex sensing analysis of radially and pseudo-radially polarized beams

Jeffrey A. Davis[a] Don M. Cottrell,[a] Brandon C. Schoonover,[a] Johnathan B. Cushing,[a] Jorge Albero,[b] and Ignacio Moreno[b]
[a]San Diego State University, Physics Department, San Diego, California 92182-1233
[b]Universidad Miguel Hernández, Departamento de Ciencia de Materiales, Óptica y Tecnología Electrónica, 03202 Elche, Spain
E-mail: i.moreno@umh.es

Abstract. We present a simple method to check the exact realization of a radially polarized light beam by means of a vortex-sensing diffraction grating. The use of this grating easily allows the determination of the topological charges included in each of the two circular polarization components of the incident beam. Therefore a pure radially polarized beam can be easily distinguished from a pseudo-radially polarized beam. Experimental results are presented with radial beams generated with two different devices: a patterned radial polarizer and a specially designed liquid crystal device. © *The Authors. Published by SPIE under a Creative Commons Attribution 3.0 Unported License. Distribution or reproduction of this work in whole or in part requires full attribution of the original publication, including its DOI.* [DOI: 10.1117/1.OE.52.5.050502]

Radially polarized light beams have been receiving a great deal of attention, especially because they can produce very small focal spots or generate longitudinal electric field components upon focalization.[1] They can be produced using a variety of techniques, including interferometric systems,[2] optical processing systems,[3] specially designed subwavelength structures,[4] radially patterned polarizers,[5] liquid crystal devices,[6,7] or inhomogeneous birefringent elements named q-plates.[8] Commercial solutions are available. However, not all of these approaches create pure radially polarized beams.

Figure 1(a) shows the directions of the electric field associated with a pure radially polarized beam. Here, the orientation of the electric field is equal to the angle ϕ representing the azimuthal angle. The closely related azimuthally polarized beam is obtained from the radial polarization by rotating the electric field by 90 deg.[5] By contrast, Fig. 1(b) shows one example of a pseudo-radially polarized beam. In this case, the electric field vectors in the lower half have a π phase shift that reverses the directions of the electric fields toward the center rather than radially outward.

Radially polarized light is typically detected with the aid of a linear polarizer.[6,7] A dark radial line appears in the azimuthal angle denoting the direction perpendicular to the transmission axis of the analyzer. As the analyzer rotates this dark line also rotates. However, this simple measurement, as well as other more sophisticated polarimetric measurement techniques, cannot differentiate between the two polarization states shown in Fig. 1. Therefore, a simple system to detect the presence of this additional azimuthal phase can be useful as a test for the correct generation of the radial beam.

The pure radially polarized light beam of Fig. 1(a) is defined in terms of its Jones vector as

$$J_{\text{rad}} = \begin{pmatrix} \cos\phi \\ \sin\phi \end{pmatrix}. \tag{1}$$

The radial polarization converter (RPC) from ARCOPTIX is a commercial device that produces this kind of beam.[9,10] We noted in Ref. 10 that this radially polarized beam can be regarded as the following decomposition:

$$\begin{aligned} J_{\text{rad}} &= \begin{pmatrix} \cos\phi \\ \sin\phi \end{pmatrix} = \begin{bmatrix} \frac{1}{2}\left(e^{i\phi} + e^{-i\phi}\right) \\ \frac{-i}{2}\left(e^{i\phi} - e^{-i\phi}\right) \end{bmatrix} \\ &= \frac{e^{i\phi}}{2}\begin{pmatrix} 1 \\ -i \end{pmatrix} + \frac{e^{-i\phi}}{2}\begin{pmatrix} 1 \\ +i \end{pmatrix}. \end{aligned} \tag{2}$$

This shows that the pure radially polarized beam can be considered as the sum of a left circularly polarized beam with an spiral phase pattern with topological charge $q = +1$, plus the opposite right circularly polarized beam with another spiral phase pattern with the opposite topological charge $q = -1$.

Next we compare the analysis with a pseudo-radially-polarized beam as shown in Fig. 1(b). One commercially available device for producing these beams is a radial polarizer consisting of a set of patterned angular sectors and commercialized by CODIXX.[5,11] The Jones matrix of such a device can be expressed as

$$\mathbf{P}_{\text{rad}} = \begin{pmatrix} \cos^2\phi & \sin\phi\cos\phi \\ \sin\phi\cos\phi & \sin^2\phi \end{pmatrix}. \tag{3}$$

If right circularly polarized light is used to illuminate this device, the output is given by

$$J_{\text{out}} = \mathbf{P}_{\text{rad}} \cdot \frac{1}{\sqrt{2}}\begin{pmatrix} 1 \\ +i \end{pmatrix} = e^{i\phi}\begin{pmatrix} \cos\phi \\ \sin\phi \end{pmatrix}, \tag{4}$$

i.e., it generates the radially polarized beam in Eq. (1) but with an additional spiral phase pattern. We call this as the pseudo-radially polarized beam. A similar beam is generated
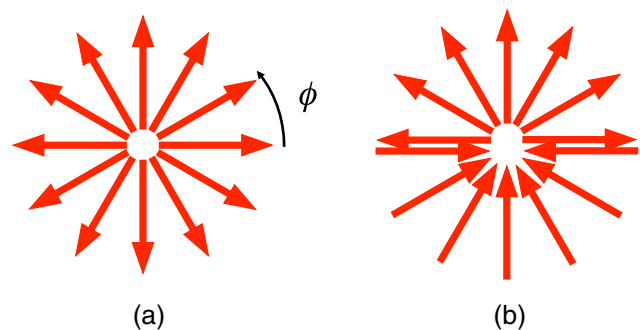
Fig. 1 Electric field vector directions for (a) pure radial polarization and (b) pseudo-radial polarization.

with the liquid crystal based system in Ref. 7. Following the decomposition in Eq. (2), we can rewrite this beam as

$$J_{\text{out}} = \frac{e^{i2\phi}}{2}\begin{pmatrix} 1 \\ -i \end{pmatrix} + \frac{1}{2}\begin{pmatrix} 1 \\ +i \end{pmatrix}. \qquad (5)$$

Note than now the right circularly polarized component of the beam carries no spiral phase (with $q = 0$), while the left circularly polarized component carries a spiral phase term with topological charge $q = +2$. A similar result would be obtained if the system were illuminated with left-handed circular polarized light. However, now the left circularly polarized component will carry no spiral phase while the right circularly polarized component will carry a spiral phase term with topological charge $q = -2$.

As stated earlier, it is difficult to easily differentiate between the two radially polarized beams in Fig. 1 because intensity measurements are insensitive to the additional phase terms. In previous work,[12] we proposed a vortex sensing diffraction grating that, as we show here, is well suited for the identification of these two polarization states.

We briefly review this vortex grating analyzer approach, and more details are found in the references.[12,13] We first form the product $V_\ell(\phi)G_\gamma(x)$ of a two-dimensional (2-D) vortex producing phase pattern $V_\ell(\phi) = \exp(i\ell\phi)$ with a linear phase diffraction grating pattern $G_\gamma(x) = \exp(i\gamma x)$. Here x is the horizontal spatial coordinate, $\gamma = 2\pi/d$ where d is the period of the grating and the variable ℓ represents the topological charge of the vortex producing phase pattern. The result is a forked type phase grating.[14] Next we form a binary phase-only phase pattern so that all phase values above a threshold level are given the phase value of π and all those below the phase level are given a phase value of 0. This yields a new grating that can be represented by a Fourier series as

$$G_{\ell,\gamma}(x,y) = \sum_{n=-\infty}^{\infty} c_n \exp(i\ell n\phi)\exp(in\gamma x). \qquad (6)$$

When we form the Fourier transform of this product in the focal plane of a lens, each focus at a location $p = n\gamma$ is characterized by a vortex beam having a charge of ℓn and intensity determined by $|c_n|^2$.

Next, we illuminate this diffraction grating with a scalar vortex beam represented here by $\exp[im\phi]$ [such as those composing the radially polarized beams in Eqs. (2) or (5)]. Now this product is represented by $\sum_{n=-\infty}^{\infty} c_n \exp[i(m+\ell n)\phi]\exp(in\gamma x)$. When we form the Fourier transform of this product, each focus spot at a location $p = n\gamma$ is characterized by a vortex spot having a charge of $m + \ell n$. For values of $m = -\ell n$, the n'th diffracted order will be characterized by a delta function. So the existence of a delta function on the n'th diffraction order indicates the illumination by a vortex beam of charge $m = -\ell n$. Note that this technique can be used for either integer or fractional values of ℓ (Ref. 13).

The intensity of each delta function is determined by the square modulus of the coefficients in the Fourier series in Eq. (6). The values for these coefficients $|c_n|^2$ depend on the encoding technique. In previous work, we have used three approaches. First, we employed binary π phase gratings (i.e., with values ± 1) where we varied the width (w) of the

+1 region compared with the grating period (d).[12] In a second approach, we obtained equal values for the coefficients by using a Dammann grating approach.[15] Finally, we utilized a new approach where the coefficients could be varied such that the higher charges had a greater coefficient[16] by applying the theory for the optimal phase beam splitters.[17]

In this work we apply this vortex sensing technique to test the purity of the incident radially polarized beam. Note that the above described approach is a scalar approach. Therefore, we have to consider the decomposition in Eq. (2) and analyze the two different circular polarization components. For this purpose we encoded the vortex sensing grating onto a transmissive parallel-aligned liquid crystal display (LCD) manufactured by Seiko-Epson, with 640×480 pixels and pixel spacing of $\Delta = 42~\mu$m, and a phase modulation range exceeding 2π radians.[18] For this example, following the method in Ref. 15, we encoded a Dammann vortex grating. This type of design allows encoding a number of orders with equal intensity (thus providing equal level of detection) and can be reproduced in binary devices. The grating was designed to generate five equally intense beams in the positions of the 0th, $\pm 1^{\text{st}}$ and $\pm 2^{\text{nd}}$ diffraction orders. The vortex sensing grating is selected with topological charge $\ell = 1$.

We begin by illuminating the vortex grating with a plane wave that is linearly polarized parallel to the LC director axis. Then the Fourier transform is captured in the back focal plane of a converging lens. Results are presented in Fig. 2(a). A bright spot corresponding to a delta function is recovered
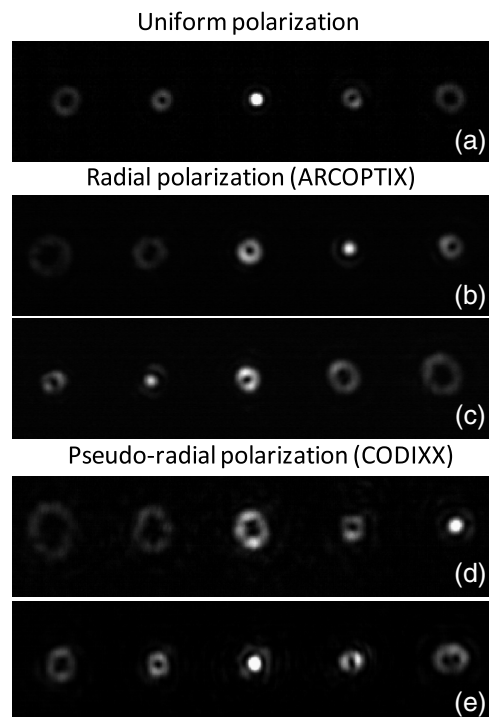
Fig. 2 Experimental results formed in the Fourier transform plane, (a) vortex grating analyzer illuminated with a plane-wave; (b) and (c) are obtained when the ARCOPTIX device is incorporated, producing the pure radially polarized beam; (d) and (e) are obtained when the CODIXX polarizer is incorporated, producing the pseudo-radially polarized beam; (b) (d) and (c) (e) correspond with the left and right circular polarization components selected, respectively with RCP and LCP films.

at the 0'th order. Vortex beams are generated on ± 1'st and ± 2'nd diffracted orders, with topological charges ± 1 and ± 2, respectively. When focused in the Fourier plane, they create doughnut focalizations, with increased diameter as the absolute value of the topological charge increases (and thus the energy in higher orders is distributed across a wider area).

Next we test the radially polarized beam produced with a radial polarization converter (RPC) from ARCOPTIX.[9] This device has a twisted nematic LC polarization rotator cell having an entrance plate with a linear director axis and an exit plate having a circularly rubbed director axis.[10] The liquid crystal molecules rotate the polarization state of the incident light clockwise between the two plates in the upper half of the device and counterclockwise in the lower half. This causes a π phase step in the center of the beam, which is removed using the half-plane retarder cell. As a result, a pure radial polarization is obtained. In order to apply the vortex grating analyzer to this device, we first illuminated the grating displayed on the LCD. The ARCOPTIX device is placed right after the LCD. A half wave-plate is also included in between to rotate the vertically polarized output from the LCD to the horizontal polarization required by the ARCOPTIX device to generate radially polarized light. In order to differentiate between the polarizations of the output beams, we used right and left circular polarizer films (RCP and LCP, respectively) placed in front of the detector to select the corresponding circular polarization component.

Figure 2(b) and 2(c) show experimental results. It can be seen that the bright focalization has moved to the $+1$ diffraction order for one circular component, while it moves in the opposite sense for the other circular component. This is in agreement with Eq. (2), thus verifying that this device generates a pure radially polarized beam. Note also that in each case, the zero order appears with the doughnut focalization characteristic of charge $\ell = 1$.

Next we show results using a radial polarizer produced by CODIXX.[5,11] This device consists of a set of patterned angular sectors, where each segment produces polarized light at different radial angles. These devices are designed to be illuminated with either unpolarized light or with either LCP or RCP light. We used a similar experimental configuration as above. We first illuminated the grating displayed on the LCD with linearly polarized light. The output from the LCD is still linearly polarized. We generated circularly polarized light by placing a quarter waveplate after the LCD. This was followed by the CODIXX device placed right after the LCD. In order to differentiate between the polarizations of the output beams, we again used right and left circular polarizer films (RCP and LCP, respectively) placed in front of the detector to select the corresponding circular polarization component. Experimental results are shown in Fig. 2(d) and 2(e). In this case, the bright focalizations appear on the zero and second order respectively, for each of the two circular components. This is now in agreement with Eq. (5), showing that the beam generated with this device is a pseudo-radial polarization. When we illuminated the CODIXX device with left circularly polarized light, the bright focalizations appeared on the zero and minus second order with the correct circular polarizations as predicted. These photos are not shown for brevity.

In conclusion, we demonstrated that vortex gratings are useful to distinguish a pure radial beam from a pseudo-radial beam. We provided analythical expressions for a linear decomposition of these beams on a basis of circular polarization components. These decompositions showed that radial or pseudo-radially light can be detected by analyzing the vortex content on each circular polarization component. This is demonstrated since the response in the Fourier transform plane after the grating varies when illuminating the LCD with radial or pseudo-radial light analyzed with left and right circular polarizers. We analyzed the radially polarized light generated with two commercially available devices (the liquid crystal device manufactured by ARCOPTIX, and the patterned radial polarized manufactured by CODIXX). We proved that the first device generates a pure radial polarization, while the second one generates a pseudo-radial polarized beam when illuminated with circular polarized light. The CODIXX polarizer can thus be used to generate pure radial polarization, but an additional spiral phase pattern must be added.

We believe that these results will be useful for the optics community.

Acknowledgments

References

1. S. Quabis et al., "Focusing light into a tighter spot," *Opt. Commun.* **179**(1), 1–7 (2000).
2. N. Passilly et al., "Simple interferometric technique for generation of a radially polarized light beam," *J. Opt. Soc. Am. A* **22**(5), 984–991 (2005).
3. C. Maurer et al., "Tailoring of arbitrary optical vector beams," *N. J. Phys.* **9**, 78 (2007).
4. Z. Bomzon, V. Kleiner, and E. Hasman, "Formation of radially and azimuthally polarized light using space-variant subwavelength metal stripe gratings," *Appl. Phys. Lett.* **79**(1), 1587–1589 (2001).
5. I. Moreno et al., "Polarization manipulation of radially polarized beams," *Opt. Eng.* **51**(12), 128003 (2012).
6. M. Stalder and M. Schadt, "Linearly polarized light with axial symmetry generated by liquid-crystal polarization converters," *Opt. Lett.* **21**(23), 1948–1950 (1996).
7. J. A. Davis et al., "Two-dimensional polarization encoding with a phase-only liquid crystal spatial light modulator," *Appl. Opt.* **39**(10), 1549–1554 (2000).
8. F. Cardano et al., "Polarization pattern of vector vortex beams generated by q-plates with different topological charges," *Appl. Opt.* **51**(10), C1–C8 (2012).
9. "Radial polarisation converter," http://www.arcoptix.com/ (9 May 2013).
10. I. Moreno et al., "Decomposition of radially and azimuthally polarized beams using a circular-polarization and vortex-sensing diffraction grating," *Opt. Express* **18**(7), 7173–7183 (2010).
11. "Patterned polarizer," http://www.codixx.de/cms/polarizers/codixx.html (9 May 2013).
12. I. Moreno et al., "Vortex sensing diffraction gratings," *Opt. Lett.* **34**(19), 2927–2929 (2009).
13. N. Zhang et al., "Analysis of fractional vortex beams using a vortex grating spectrum analyzer," *Appl. Opt.* **49**(13), 2456–2462 (2010).
14. V. Y. Bazhenov, V. Vasnetsov, and M.S. Soskin, "Laser beams with screw dislocations in their wavefronts," *JETP Lett.* **52**(8), 429–431 (1990).
15. I. Moreno et al., "Encoding generalized phase functions on Dammann gratings," *Opt. Lett.* **35**(10), 1536–1538 (2010).
16. J. Albero et al., "Generalized phase diffraction gratings with tailored intensity," *Opt. Lett.* **37**(20), 4227–4229 (2012).
17. L. A. Romero and F. M. Dickey, "Theory of optimal beam splitting by phase gratings. I. One-dimensional gratings," *J. Opt. Soc. Am. A* **24**(8), 2280–2295 (2007).
18. J. A. Davis et al., "Transmission variations in liquid crystal spatial light modulators caused by interference and diffraction effects," *Opt. Eng.* **38**(6), 1051–1057 (1999).